Density-Based Phase-Separation Asymmetric Polyethylene–Poly(Dimethyl Siloxane) Blend Membranes: Preparation and Properties

Pratibha Pandey,[1] R. S. Chauhan,[1] R. P. Semwal,[1] S. Banerjee,[1] Rajeev Jain[2]

Defense Research and Development Establishment, Jhansi Road, Gwalior, Department of Chemistry, Jiwaji University, Gwalior 474002, India

Received 27 September 2003; accepted 22 July 2003

ABSTRACT: A new concept of density-based phase separation for the preparation of asymmetric membranes from polyethylene (PE) blended with liquid poly(dimethyl siloxane) (PDMS) has been tried. The PE/PDMS membranes were prepared via high-temperature solution casting. The purpose of incorporating PDMS was to utilize its flexibility, relatively high density in comparison with PE, and dissolution in common solvent for the formation of asymmetric PE/PDMS membranes. The study has been carried out with 1.25, 2.5, 5, and 10% (v/w) loading of PDMS. A host of techniques were used to study morphology of PE/PDMS blend membranes. The membranes show nodular structure on surfaces in contact with solvent vapor environment, whereas the opposite surfaces have smoother texture devoid of nodules. Although differential scanning calorimetric (DSC) melting endotherms indicate enhancement of crystallinity with PDMS addition, chemical etching and subsequent scanning electron microscopic (SEM) observations show increasingly ordered spherulitic pattern on individual nodules with the incorporation of PDMS up to 2.5%. The density of the films also increases with the addition of PDMS as compared to the control. ATR-FTIR data revealed asymmetric distribution of PDMS in membranes with more PDMS retention toward lower surface of membranes. Membrane cross sections were indicative of graded porosity with increasing pore size toward the bottom surface of membranes. The results were explained in terms of density-based phase separation. © 2003 Wiley Periodicals, Inc. J Appl Polym Sci 91: 2278–2287, 2004

Key words: PE : PDMS blend; nodules; asymmetric PE membrane; spherulites; gas separation

INTRODUCTION

Over the past two decades, many novel materials as well as preparation methods have been developed to prepare membranes for material separation.[1–3] Polymer blends can be of great practical interest because a range of useful membrane materials can be produced by blending existing polymers. Polymer–polymer interaction can strongly influence not only the transport properties of the blends but also improves their mechanical properties. Given that most blends are partially miscible, the challenge of predicting the properties of polymer blend depends on the basic structure of the components, the nature of the interfacial energy, and the type and the energy of intermolecular interaction of the blend components.[4–7] It becomes thus difficult to predict the performance of a membrane prepared by blending without actual experimentation. With this consideration, the transport properties of gases in both homogeneous and heterogeneous blends have been explored.[7–9] In heterogeneous blends, the morphology of the biphasic structure and the nature of the interface are the main factors that govern the transport properties of gases, whereas for homogeneous blends, the permeation and selectivity behavior of the membranes depend to a large extent on their physical properties.

It is known that asymmetric membranes perform better in terms of selectivity and improved permeability as compared to the dense membranes.[1–2] In industrial applications, other than microfiltration, symmetrical membranes have been displaced almost completely by asymmetric membranes which have higher fluxes. The phase-inversion casting method intrinsically produces asymmetric structures. The method allows the tailoring of a distinct functional structure by varying the casting solution composition and casting conditions. Asymmetric polymer membranes, prepared by the phase-inversion technique, usually have a top dense layer, consisting of closely packed nodular structure, and a porous support structure throughout the bulk of the membrane.[10]

Polyethylene (PE) has been widely investigated, from scientific as well as industrial interest as a membrane material.[11] The formed membranes are dense and have low permeability. It is important to incorporate asymmetric structure in such polymers which are inert to chemicals, relatively inexpensive, and easily

Correspondence to: R. S. Chauhan (drde@sancharnet.in).

Journal of Applied Polymer Science, Vol. 91, 2278–2287 (2004)

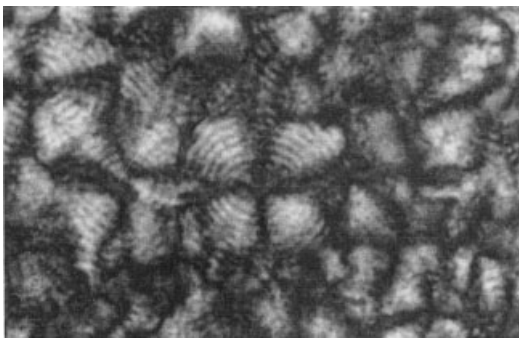

Figure 1 Concentric spherulites of polyethylene observed in the optical microscope between crossed polarizers (×1000).

available. The solution-blend-casting method can be of practical help to explore the possibility of preparing asymmetric membrane. There can be two types of blend membranes: one in which both polymers are retained in the end-use material and both contribute to the properties of the membrane, and the other in which one of the components is removed during the formation of the membrane and acts only as a pore former.[12] Poly(ethylene glycol) has been used as a pore former in regenerated cellulose microporous membranes.[13] There are, however, only a few reports describing the effect of polymer addition on structure and pore formation in polymeric membrane by using the blend solution method.[13,14] The thermally induced phase-separation method also has been in vogue for the preparation of microporous polypropylene (PP)/PE membrane by using high boiling liquid component as pore former.[15]

The present article deals with a novel method of preparing an asymmetric membrane of polyethylene blended with poly(dimethyl siloxane) (PDMS). PE is less expensive, inert to chemicals, and easily available. An incompatible PDMS having higher density (0.97) than PE (0.93) was used as pore former to facilitate the formation of porous support beneath the top PE dense layer, so as to improve the mass transfer properties.[16] In the present case, PDMS was used to prepare membranes having varying add-on. The resulting morphology was studied by employing a host of techniques such as chemical etching, FTIR, differential scanning calorimetry (DSC), and scanning electron microscopy (SEM).

EXPERIMENTAL

Membrane preparation

Materials

PE membranes were prepared by dissolving commercially available low-density (0.93) PE granules (3 wt % solution) at 100°C in toluene. PDMS was purchased from Aldrich (d 0.97, bp > 149°C, viscosity 120 cst) and was used as received. Analytical-grade toluene was used as a solvent. Methanol and carbon tetrachloride (AR, Merck) were used for density measurement. H_2SO_4 (AR, Qualigen) and 30% H_2O_2 (Merck), acetone (AR, Merck), and potassium permanganate (AR, SD Fine Chemicals) were used for chemical etching.

Methods

Both PDMS and PE are soluble in toluene at 100°C and form a well-dispersed homogenous mixture. A series of PE : PDMS blend membranes was prepared by mixing 1.25, 2.5, 5, and 10% PDMS by volume with PE at 100°C. The membranes were cast at 100°C in an oven on a 24 × 24 cm glass plate having raised boundaries. The glass plate was covered soon after pouring the polymer solution to slow down the evaporation of solvent from the film. This ensured uniform spreading of solution under saturated toluene atmosphere. The dilute casting solution was then allowed to evaporate at 100°C in a closed oven for 24 h. As the solvent evaporated, demixing of PE and PDMS occurred and PE gradually started solidifying. The formed membranes were washed in water and subsequently dried

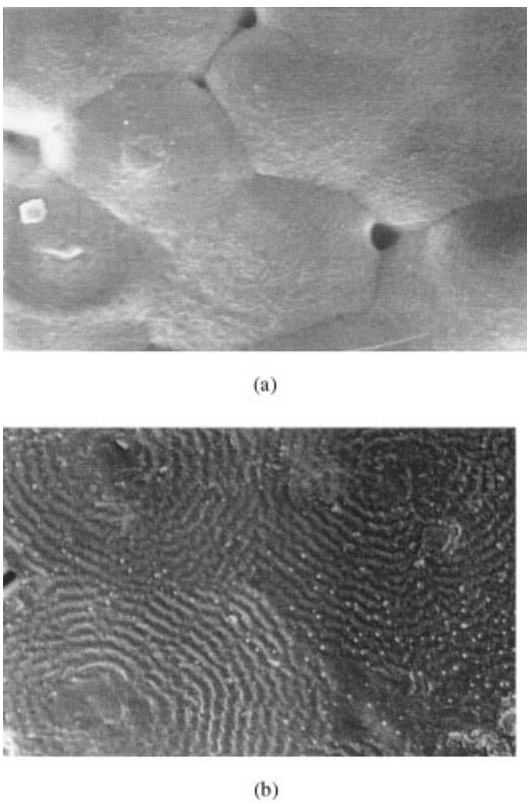

Figure 2 (a) Surface of polyethylene film presenting structureless relief (×1500). (b) Surface of polyethylene film after paramagnetic etching showing concentric rings of spherulites (×2500).

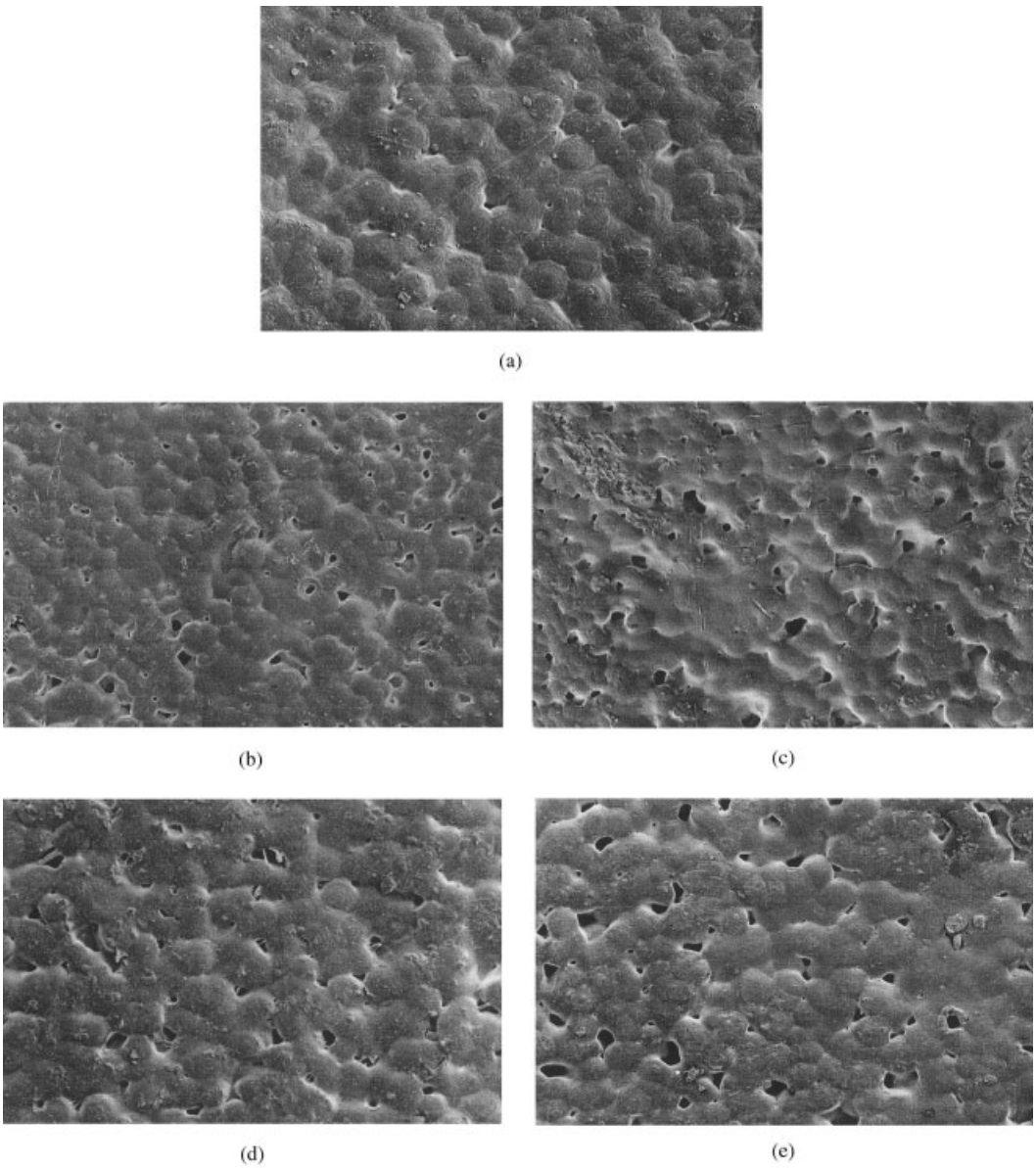

Figure 3 (a–e) Electron micrograph of polyethylene and PE : PDMS films showing nodular structure on the top surface at various add-ons (×250).

for 3 days at 95°C and then used for permeation tests and characterization. The membrane thickness varied from 40 to 60 μm. In the present study, no attempt was made to measure the actual PDMS contents in the formed films. The data are presented in terms of PDMS add-on.

Chemical etching

Membrane specimens were subjected to permanganic etching.[17] The etching protocol was modified in terms of temperature as well as duration for the present work. The controlled etching revealed the spherulitic pattern of nodules present on the top surface. A 7% w/v solution of $KMnO_4$ in concentrated H_2SO_4 was prepared. The specimens were etched at 0°C for 10 min. The membranes were washed for 5 min with 2 : 7 H_2SO_4 distilled water cooled to −20°C. The samples were then kept in acetone for 5 min and dried at room temperature for 24 h.

Density determination

Density of PE and PE : PDMS blend membrane was determined by the floating method by using spectroscopy-grade carbon tetrachloride ($d = 1.592$) and methanol ($d = 0.791$). A known volume of carbon tetrachloride was taken in a graduated cylinder. A film specimen was introduced in the liquid. Being lighter than carbon tetrachloride, the film specimen floated on the

TABLE I
Variation in Size and Shape of Nodules with the Addition of PDMS in PE Membrane

PDMS (%)	No. of nodules unit area	CV %	No. of readings	X major axis (μm)	CV %	Y minor axis (μm)	CV %	Y/X Circularity
0	270	12.0	44	46	6.8	35.46	4.4	0.77
1.25	287	10.0	90	46	5.23	38.52	6.13	0.85
2.5	309	10.3	48	27	3.34	23.03	3.18	0.84
5	246	9.0	50	44	3.31	42.50	4.2	0.96
10	238	14.0	60	43	5.0	41.50	5.3	0.97

surface. Methanol was added gradually with constant stirring until the specimen followed a Brownian motion, indicating that the density of specimen equals that of the liquid mixture. All the experiments were conducted in a controlled atmosphere. Care was taken to reduce the solvent evaporation during testing. Density was calculated by computing mass and volume of two liquids. d_1V_1, d_2V_2 correspond to the mass of CCl_4 and methanol and V_1, V_2 correspond to their volumes, respectively.

Optical microscopy

Surfaces of the PE control as well as chemically etched membranes were examined under a polarizing optical microscope Leica DMLP to study the spherulitic pattern of the membrane as well as the general morphology.

Fourier transform infrared

Fourier transform infrared spectroscopy (FTIR), in combination with the attenuated total reflection (ATR) technique, was used to characterize the distribution of PDMS across the membrane thickness. Spectra of pure PE and PDMS were also taken as reference. FTIR scans of film surfaces (top and bottom) were taken on a Perkin–Elmer $\times$1720 model spectrometer by using the ATR technique. The crystal used was KRS-5, having a refractive index (RI) of 2.4. The IR spectral range was taken between 2000 and 450 cm^{-1}, which covered the characteristic group frequency range for PE and PDMS polymers. One hundred scans at 4 cm^{-1} resolution were taken for each spectrum.

Differential scanning calorimetry

DSC scans were taken on a TA Instruments DSC 2920 by using indium as standard. The scans were taken at a heating rate of 10°C per minute in a nitrogen atmosphere from 40 to 150°C. The sample size was kept between 4 and 6 mg.

Scanning electron microscopy

The surface relief of solvent-cast films before and after etching was observed under a JSM-840 Jeol scanning electron microscope at 5 kV after coating the specimens with a thin layer of gold in a JFC-1100 sputter-coating unit. Cryofractured surfaces (obtained by dipping in liquid nitrogen and fracturing by hand) were also studied to examine the internal structure as well as the pore size and their distribution in the membranes. Various structural parameters, such as nodule size and pore diameters, were recorded directly from the screen of the microscope by tracing them on a transparent sheet at various magnifications. Nodules were counted from micrographs at $\times$250 magnification. Two regions were selected for recording the pore size as well as number distribution in the membrane cross sections: one toward the top and the other toward the bottom surface at $\times$1500 magnification. The top represented approximately the upper two-third membrane thickness, while bottom side represented one-third of the remaining area of the membrane. The circularity of nodules was calculated by dividing the values of minor axis with the major axis.

Permeation measurement

Permeation measurements were done for oxygen, nitrogen, and hydrogen on a DRDE-made permeation assembly coupled to a soap-bubble permeation measurement device. All experiments were carried out at 27 $\pm$ 2°C. The area of the test membranes was kept at 12.75 cm^2.

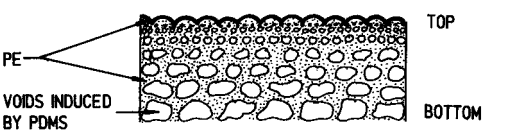

Schematic presentation of graded pore size induced by PDMS in polyethylene matrix due to density based phase separation.

Figure 4 Schematic presentation of asymmetric PE : PDMS membrane showing graded porosity.

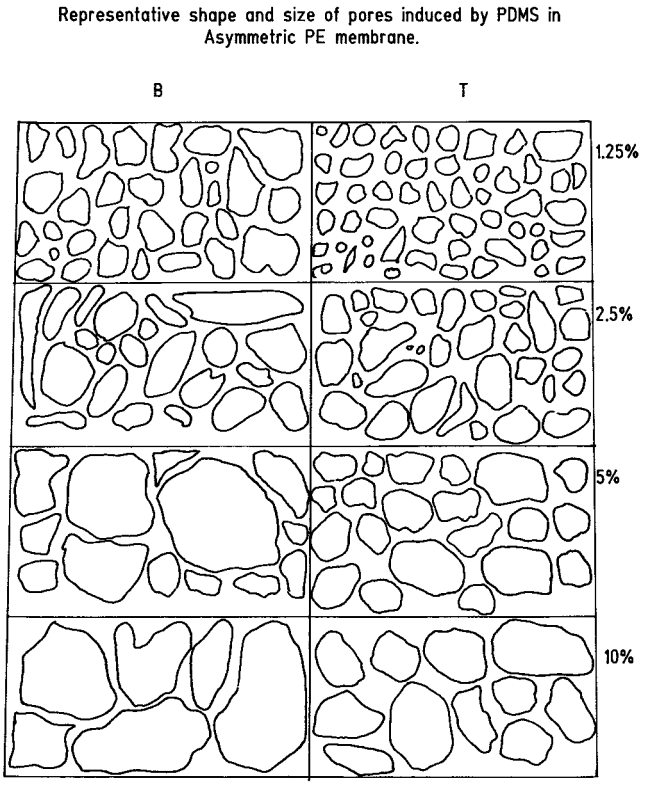

Figure 5 Representative tracing of size and shape of pores in membrane cross sections (×1500).

RESULTS AND DISCUSSION

Figure 1 presents the photomicrograph of PE film taken on a polarizing microscope. It shows concentric fringes and their arrangement in the spherulites. Figure 2(a) shows the surface relief of PE film having interconnected nodules. The surface is devoid of any structural details. Figure 2(b) represents a similar surface after permanganic etching. The etching brings out the spherulitic structure present on the nodules. These fringes became more distinct and well defined up to 2.5% PDMS add-on. Although this basic structure was present in all the membranes, the distinctness or the sharpness between fringes became diffuse with further PDMS addition.

TABLE II
Size and Number of Pores in Membrane Cross-Section Induced by PDMS in PE/PDMS Asymmetric Membrane

% PDMS	Region[a]	Sizes (μm)	Average no. of pores
1.25	Top	1.09	21.12
	Bottom	1.19	23.75
2.5	Top	1.05	18.7
	Bottom	1.23	34.1
5.0	Top	1.67	31.1
	Bottom	2.55	46.7
10.0	Top	2.62	NM
	Bottom	3.53	NM

[a] Top, two-third area of the upper part of membrane; bottom, one-third area of the lower part of membrane; NM, not measured.

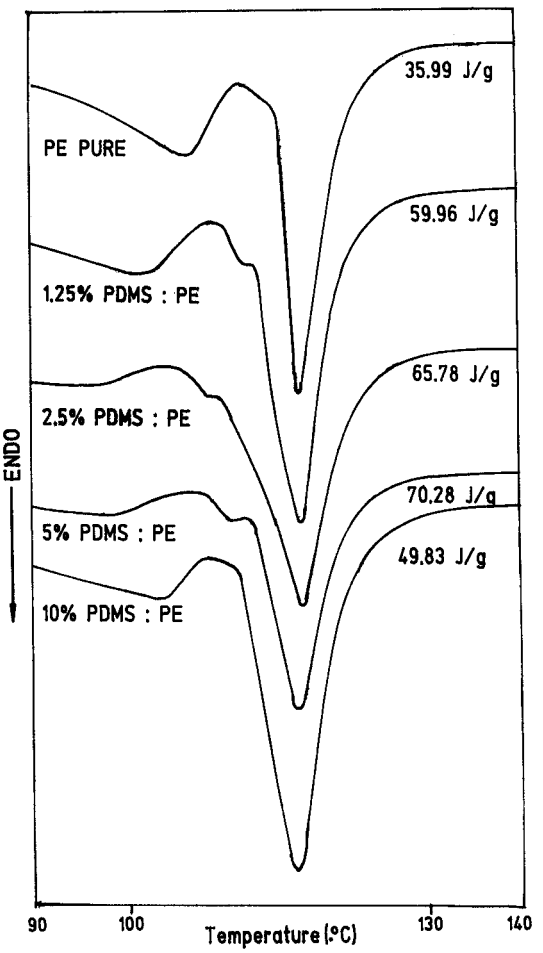

Figure 6 Melting endotherms of PE and PE : PDMS blend membranes.

Figure 3 shows the surface relief of solution-cast PE as well as PDMS-blended PE membranes, after permanganic etching, at ×250 magnification. Although the gross morphology appears similar, in that all the specimens show nodular structure covering the entire top surface, there are subtle morphological variations, which resulted from the blending of various concentrations of PDMS.

The surface nodules are circular in shape and contiguous. However, in places the internodular distance was wide enough to create a discontinuity. There is a consistent increase in the internodular gap with the increase in the addition of PDMS from 1.25 to 10%. It was observed that the number of nodules per unit area tends to increase consistently with the increase in PDMS concentration up to 2.5% add-on, from 270 for pure PE membrane to 309 for 2.5% add-on (Table I). Thereafter, the number of nodules decreased drasti-

TABLE III
Melting Temperature (T_m), Melting Energy (ΔH), Percent Crystallinity, and Density of Various PE/PDMS Blend Membranes

PDMS (%)	T_m (°C)	ΔH (J/g)	Crystallinity[a] (%)	Density
0	117.31	35.99	12.41	0.9596 ± 0.0007
1.25	114.68	59.16	20.40	0.9682 ± 0.0020
2.5	115.45	65.78	22.68	0.9715 ± 0.0018
5.0	115.13	70.28	24.23	0.9661 ± 0.0020
10.0	116.45	49.83	17.18	0.9658 ± 0.0032

[a] Δ H/290, Heat of fusion of pure PE crystal taken as 290 J/g.[20]

cally from 309 for 2.5% PDMS to 246 for 5% PDMS and 238 for 10% add-on. Concurrent to changes in the number of nodules, there is a corresponding change in the size of the nodules. The average size of the nodules in the PE was found to be 46 μm: the size reduced to 27 μm on addition of 2.5% PDMS. Then, the size again increased to 44 μm for 5% PDMS add-on. It is interesting to note that the circularity of the nodules increased with PDMS add-on: the circularity increased from 0.77 for PE films to 0.97 for the 10% PDMS add-on. All these indicate that PDMS influences the morphology of blend in more than one way. It is known that the properties of the pore former play an important role in the formation of the morphology.[13] The formation of spherical nodular structure is perhaps the result of combined effects of shrinkage, due to evaporation of solvent from the surface, and the resulting surface tension forces. The change in the number and corresponding increase in size of nodules can be attributed to the presence of PDMS in the PE matrix up to a particular concentration. It appears that PDMS perhaps acts as a nucleating agent up to a particular concentration where it may be present in well-dispersed, isolated microscopic droplets and induces the above morphological responses. It is well known that, in a heterogeneous blend, the nucleation starts on surfaces, cavities, and other impurities of the insoluble polymer and all these help to an extent for the enhancement of the crystallinity.[5] With increased volume fraction of dispersed PDMS phase smaller PDMS droplets will coalesce, resulting in the formation of larger drops which will result in the phase exclusion of added PDMS either to interspherulitic area enclosed by the nodules creating internodular gaps and discontinuity or even to migrate out of the membrane at higher add-on. This in turn results in a lesser number of nucleating sites. Thus, comparatively fewer nodules of larger size and increasing internodular gaps are formed at higher PDMS add-on. It is reported that in a heterogeneous blend, during the earlier stages of microstructure formation, the two-phase system will continue to evolve in response to its tendency to reduce the surface energy associated with interfacial area. This process of coarsening often results in a reduction in the number of droplets and an increase in their size.[18]

The purpose of incorporating liquid PDMS in PE was to utilize its easy mixing with PE solution in toluene as well as comparatively higher density of PDMS to create density-based phase separation due to the inhomogeneity, which sets in as a result of evaporation of toluene while the membrane is formed with the intent to induce asymmetric structure. As such, PE and PDMS are not miscible, and therefore, while PE solidifies during solvent evaporation, a certain amount of PDMS will also get trapped inside the formed PE structure while the rest will segregate out. Because PE has lower density than PDMS, it was expected that, given sufficient time during membrane formation (casting was carried out in a closed environment where slow evaporation was allowed), PE would migrate to an upper layer and form a dense top layer. Subsequent layers toward the bottom surface would have various sizes of PDMS droplets (formed because of coalescence) entrapped by PE during membrane formation. Although the fully entrapped PDMS microdroplets may remain trapped in the PE matrix, most of the PDMS volume present in the interconnected channels subsequently comes out of membranes, leaving behind a hollow network of PE polymer. Figure 4 presents a representative schematic di-

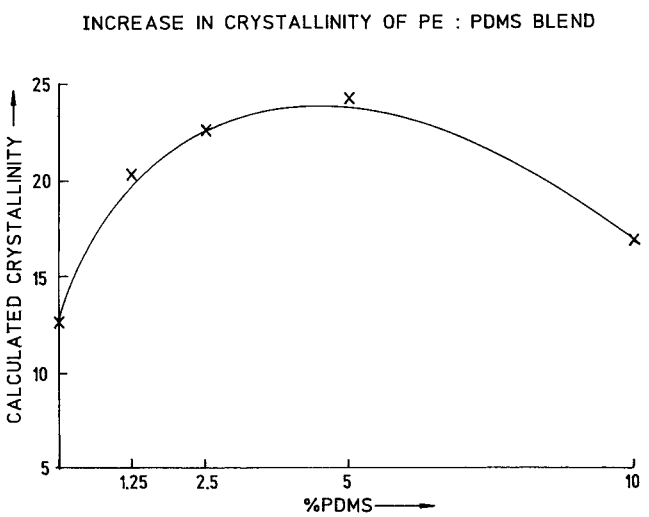

Figure 7 Effect on crystallinity with change in PDMS blend composition.

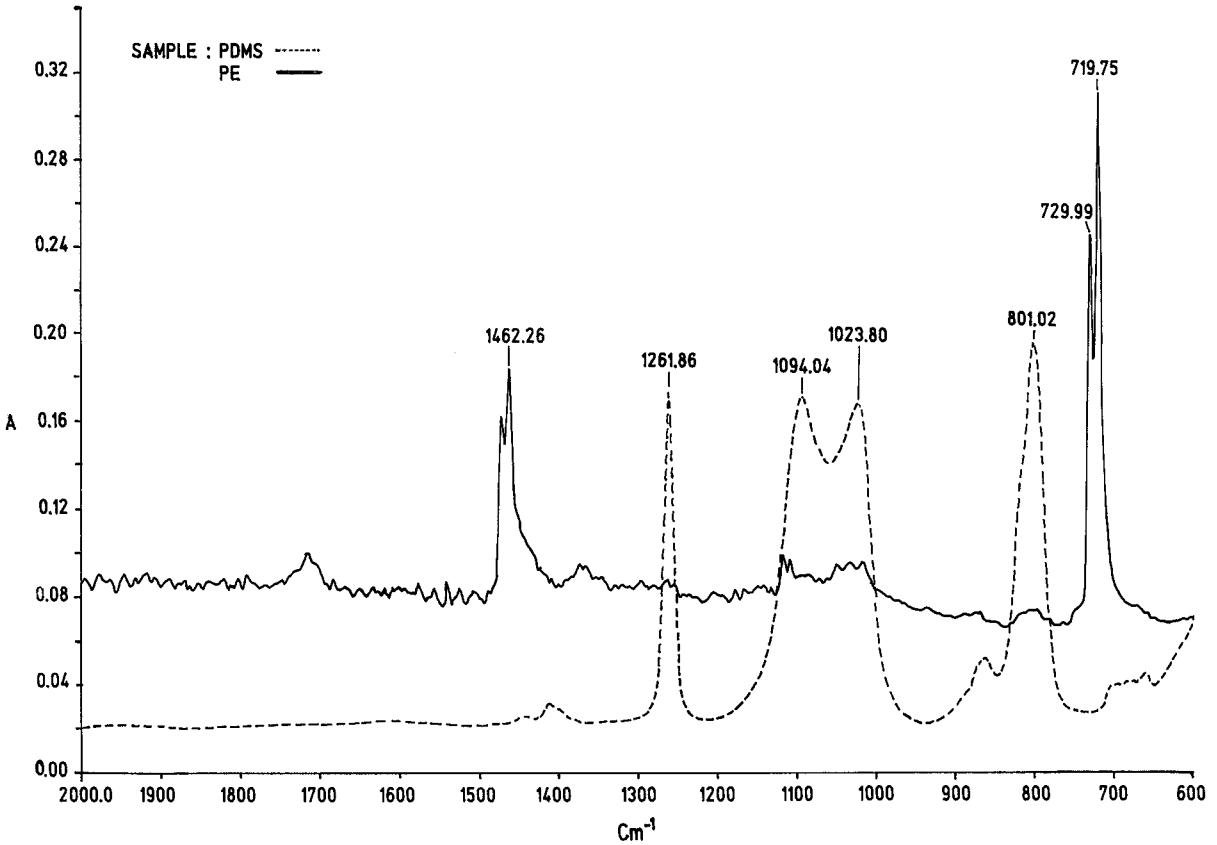

Figure 8 ATR-FTIR spectra of solvent cast polyethylene membrane and pure PDMS.

agram of such PE : PDMS films. It depicts a dense top surface and porous structure underneath. The porous structure is expected to have graded porosity because of the density-based distribution of PDMS with larger pores toward the bottom.

To confirm our reasoning, cross sections of membranes were examined in the SEM. Figure 5 shows the representative tracings of the cross section of PE : PDMS membranes having different proportions of PDMS. The figure does not represent the actual numerical density of pores present in a cross section of the membrane. However, maximum numbers of pores were drawn randomly in the figure from cross sections so as to show all shapes and sizes. It can be seen that as the percent of PDMS add-on increases from 1.25 to 10%, the size of the pores increases gradually. Also, the pores toward the bottom region are larger than those at the top. These clearly bring out the asymmetry of pore distribution in the two regions.

Table II presents the size of voids induced by PDMS in PE asymmetric membrane cross section calculated from the tracings. The voids formed near the top surface increased from 1.30 μm for 1.25% PDMS to 2.98 μm for the 10% add-on. However, the increase is steeper for the bottom part of membrane where the average pore size increased from 1.28 μm, for the 1.25% PDMS content, to 4.23 μm for 10% PDMS. The consistent increase in the size of voids, due to the addition of PDMS, clearly shows that PDMS helped in the formation of graded porosity due to gravity-induced settling of the heavier incompatible component (i.e., PDMS). The average number of pores at the two regions also shows a corresponding increase with the addition of PDMS. Thus, asymmetry again was maintained in the two regions as far as the number of pores is concerned.

Figure 6 shows the melting behavior for four compositions, namely (1.25, 2.5, 5, and 10% PDMS), along with the control solvent-cast PE membrane. PE exhibited melting at 117.3°C. All the blend compositions exhibit endotherms in a close range of temperature (between 114.68 and 116.45°C). The melting energy (ΔH) changes with blend composition and tends to increase with increasing PDMS percentage addition. In all calorimetric techniques, crystallinity is assumed to be linearly proportional to the area under the heat of fusion curves. The melting energy gradually rises from 35.99 J/g for the control to 70.28 J/g for 5% PDMS add-on. Thereafter, a sudden reduction in melting energy to a value of 49.8 J/g for 10% PDMS loading was observed. The figure also shows that the solvent-cast pure PE membrane appears to have a disordered part, which melts at a lower temperature prior to the main endotherm. However, with the ad-

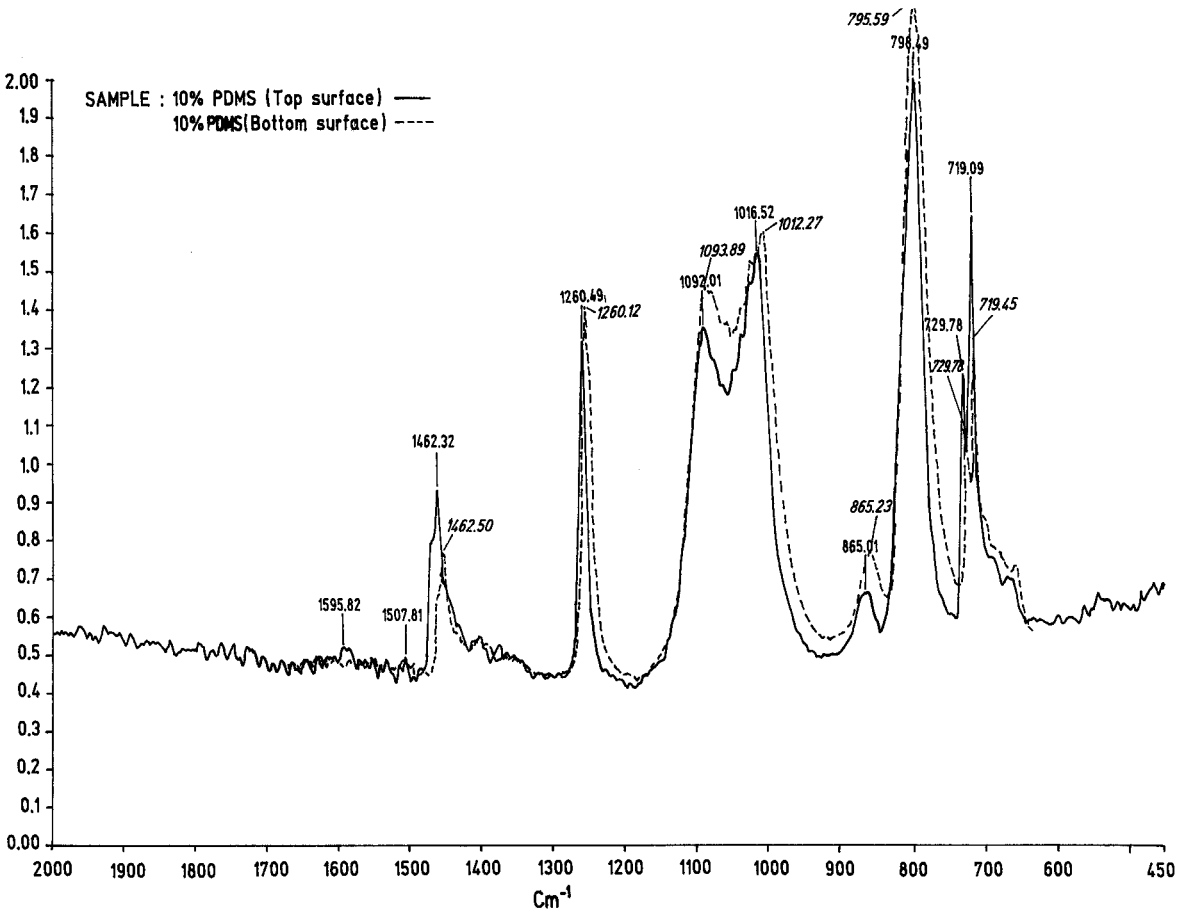

Figure 9 ATR-FTIR spectra of top and bottom surfaces of PE membrane with 10% PDMS loading.

dition of PDMS, the proportion of the less-ordered region reduced and merged into the ordered region and contributed to the melting endotherm; as a result, the melting energy registered higher values. The results of many reported experiments show that, in general, in a solvent-crystallized sample, melting occurs in the reverse order to crystallization, in that the least stable structure is that which crystallizes last and appears first in the DSC thermogram.[19]

Table III shows the melting temperature, melting energy (ΔH), percentage crystallinity, and density for the control PE and various PE : PDMS blends. [The percent crystallinity has been derived from the heat of fusion divided by the theoretical heat of fusion for pure PE crystal (290 J/g).][20] The percent crystallinity of the blend registered enhancement, from a value of 12.4% for the control PE to 24.0% for the 5% PDMS add-on. It then falls to 17.2% for 10% PDMS blend.

Figure 7 shows the calculated values of percent crystallinity against PDMS add-on. It can be seen that the crystallinity gradually increases up to 5% add-on. Beyond 5% PDMS add-on, however, there is a sharp reduction in the crystallinity. Khanbatten et al.[21] have reported detrimental effects of high amorphous content in the development of crystalline structure in a blend. It is rather interesting as well as intriguing that an incompatible PDMS tends to enhance the crystallinity of solvent-cast PE membrane when the percent of loading of amorphous polymer is low. This is perhaps the first time that such a system is reported.

It can be noted that the density of the cast PE film registered a much higher density than the PE granules. The high temperature and controlled-casting methodology in the present work helped in improving crystallization of PE. The density values for blend membranes show an increasing trend with the incorporation of PDMS. The values showed a maxima for 2.5% PDMS, where it registered a value of 0.9715. The density thereafter registered a reduction for 5 and 10% add-on. The data support the grass morphological observation from SEM, which indicated a higher number of nodules per unit area up to 2.5% PDMS. The data suggest that PDMS functions as a nucleating agent, thereby increasing the density as well as crystallinity and number of nodules. DSC data showed highest crystallinity for 5% PDMS blend, whereas the gross morphology of SEM revealed an increasing number of nodules only up to 2.5% PDMS add-on. The

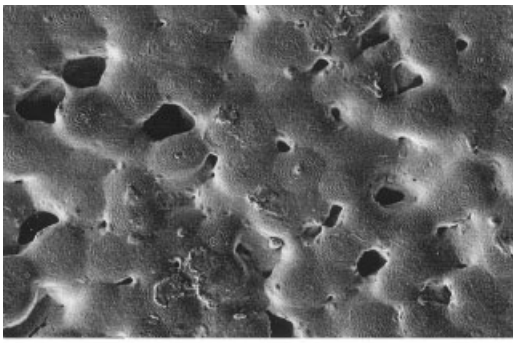

(a)

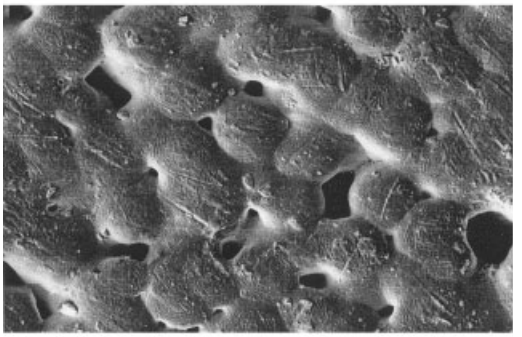

(b)

Figure 10 (a) Surface morphology of 2.5% PDMS-PE blend membrane after permanganic etching showing closely packed, circular, and well-defined spherulitic fringes (×500). (b) Surface morphology of 10% PDMS-PE blend membrane showing poorly defined spherulitic fringes (×500).

density value also showed an increasing trend up to 2.5% add-on. The reduction in crystallinity at higher PDMS content could be due to the formation of bigger clusters of PDMS droplets as a result of coalescence and segregation of the PDMS phase from PE matrix, which no longer acted as nucleation site for PE crystallites. The higher amorphous content of PDMS may also increase isolation of the individual chains of PE during crystallization, resulting in poor crystallite development as well as overall reduction in the crystallinity.

It was presumed that small entrapped PDMS droplets will remain well dispersed in the PE matrix because of high-temperature mixing, particularly at lower levels of PDMS contents in the blend. However, because of the density-based settling of PDMS droplets, a preferential distribution toward the bottom surface was also expected. To confirm the proposed mechanism, the surface ATR-IR technique was utilized.

Figure 8 shows the ATR-FTIR spectra of a solvent-cast PE membrane and of pure PDMS with their characteristic peaks. Figure 9 shows the ATR-IR spectra of PE blend membrane with 10% PDMS loading. The figure shows that the bottom layer, in contact with the glass casting surface, retains a higher amount of PDMS as indicated by the characteristic frequencies of PDMS at 1095, 1020, and 800 cm^{-1} compared to the top surface. The spectra also revealed that there is a decrease in the intensity of PE peaks (1462 and 719 cm^{-1}) at the bottom side as compared to the top surface.

Blended membranes were subjected to permanganic etching to reveal the subtle structural variation induced by the PDMS addition. Permanganic etching is highly selective and can contribute to the study of lamellar structures at high resolution. It is even possible to obtain a measure of nucleation centers.[17] Figure 10(a) shows the electron micrograph of 2.5% PDMS–PE blend membranes after 10 min permanganic etching. The micrograph reveals concentric spherulitic fringes (arrow mark) on the top surface of each nodule. The fringes are closely packed, circular, and well defined. Figure 10(b) shows the surface of 10% PDMS–PE blend membrane. The spherulitic fringes appear less ordered, poorly defined, and smooth as far as their vertical projections from the surface are concerned. Because the ordered fringes are indicative of organized crystalline phase in the nodules, it can be safely concluded that nodules of 2.5% blend are more crystalline compared to the 10% PDMS blend.

Permeation behavior

Table IV presents the permeation data for polyethylene and various blend membranes for nitrogen, oxy-

TABLE IV
Gas Permeation Data for PE and PE/PDMS Blend Membranes at Feed Pressure 8 kg/cm² at 27 ± 2°C

Composition of membrane	Thickness of membrane	Permeance (in GPU)[a]			Selectivity	
PDMS (%) in membranes	(in μm)	N_2	O_2	H_2	O_2/N_2	H_2/N_2
0	40	0.017	0.052	0.086	3.0	5.0
1.25	50	0.069	0.104	0.26	1.5	3.8
2.5	50	8.675	8.761	17.35	1.0	2.0
5.0	60	8.33	8.5	23.42	1.0	2.8
10.0	50	138.8	133.1	451.1	0.95	3.2

[a] 1GPU = 1×10^{-6} cm^3 (STP) cm^2 S cm (Hg).

gen, and hydrogen gases. The selectivity of PE for oxygen over nitrogen is 3.06 and for hydrogen over nitrogen is 5.0. The permeability of these gases increases with the increase in the PDMS contents. However, the selectivity (ratio of permeability of two gases) for these membranes decreases, as the percent loading of PDMS increases. The increase of flux in PE : PDMS blend membrane and the subsequent reduction in selectivity is the result of the pore-forming response of PDMS, which tends to reduce the overall resistance of membrane to permeation.

CONCLUSION

Blending of increasing proportions of PDMS with PE resulted in the gradual change of morphology, as revealed by the change in number and size of nodules as well as increase in size and number of the pores. The top surface of the membranes consisted of nodules having spherical shapes with a well-defined spherulitic pattern up to 2.5% PDMS add-on. The formation of spherical nodular structure is perhaps the result of a combined effect of evaporation of solvents from the surface as well as the resulting surface tensional forces and shrinkage, whereas the internodular gap resulted from the dynamics of membrane formation.

The solution blending of PE and PDMS resulted in the formation of asymmetric membrane having graded pore structure because of density-based phase separation with improved flux. Because PE has lower density than PDMS, it migrates to the upper layer during the membrane formation process. The results indicate that PDMS worked as a graded pore former. The size of the voids varied with increasing PDMS loading. The porosity gradation was from the top surface toward the bottom. The density measurements, as well as the percentage crystallinity calculated on the basis of heat of fusion, revealed that PDMS helped in significant crystallinity development in the solvent cast membranes up to a particular level of PDMS add-on. Although the addition of PDMS resulted in the formation of asymmetric structure, it could not provide a practically acceptable membrane for gas separation because of low selectivities. Attempts are being made in this laboratory to prepare thinner and superior films. However, the concept of density-based phase separation can be utilized for the preparation of asymmetric membranes by using other polymeric systems.

The authors thank K. Sekhar, Director DRDE, Gwalior for permission to publish this work. Thanks are due to Dr. Vinita Dubey for technical discussions and to U. K. S. Chauhan for typesetting the manuscript.

References

1. Baker, R. W. in Encyclopedia of Chemical Technology; Othmer, K., Ed.; Wiley: Singapore, 1995; Vol. 16; p 135.
2. Pandey, P.; Chauhan, R. S. Prog Polym Sci 2001, 26, 853.
3. Koros, W. J.; Chern, R. T. in Handbook of Separation Process Technology; Rousseau, R. W., Ed.; Wiley: New York, 1987; pp 863–953.
4. Kim, C. K.; Paul, D. R. Polymer 1992, 33, 1630, 1992, 2089.
5. Geushens, G. J Macromol. Sci, Phys 1996, B35 (3&4), 579.
6. Baker, R. W.; Blume, I. in Handbook of Industrial Membrane Technology; Porter, M. C., Ed.; Noyes Publication: Park Ridge, NJ, 1990; pp 511–580.
7. Heish, H. P. AIChE Symp Ser 1988, 84.
8. Wang, J. Q.; Li, Z. Membr Sci Tech 1998, 18, 54.
9. Tsay, C. S.; McHugh, A. J. J Polym Sci, Polym Phys Ed 1990, 28, 1327.
10. Panar, M.; Hoehn, H. H.; Hebert, R. R. Macromolecules 1973, 6, 777.
11. Othmer, K. Encyclopedia of Chemical Technology; Wiley: Singapore, 1995; Vol. 17; p 702.
12. Kesting, R. E. Polymer Solution, Synthetic Polymeric Membranes—A Structural Perspective; Wiley: New York, 1985; Chapter 5, p. 186.
13. Yang, G.; Zhang, L.; Feng, H. J Membr Sci 1999, 161, 31.
14. Yang, G.; Zhang, L.; Feng, H. J Membr Sci 1996, 114, 149.
15. Caplan, M. R.; Chiang, C. Y.; Llyod, D. R.; Yen, L. Y. J Membr Sci 1997, 130, 219.
16. Gojibus, N.; Maschke, U.; Benmoung, F.; Ewen, B.; Coquerete, X.; Benmoung, M. J Polym Sci, Part B: Polym Phys 2001, 39, 581.
17. Bassett, D. C. Principles of Polymer Morphology; Cambridge Univ. Press: Cambridge, UK, 1981.
18. Song, S.-W.; Tor Kelson, J. M. Macromolecules 1994, 27, 6389.
19. Strickland-Constable, R. F. Kinetics and Mechanism of Crystallization; Academic Press: New York, 1968.
20. Wright, K. J.; Lesser, A. J. Macromolecules 2001, 34, 3626.
21. Khanbattan, F. B.; Warner, F.; Russell, T.; Stein, R. S. J Polym Sci, Polym Phys Ed 1976, 14, 1391.
22. Shreedharamurthy, R. S.; Leyden, D. E.; D'Alonzo, R. P. Appl Spectrosc 1985, 39, 855.